

Experimental Analysis of Temperature and Crystallinity Profiles of Wood Sawdust/Polypropylene Composites During Cooling

N. Sombatsompop, A. Kositchaiyong, E. Wimolmala

Polymer Processing and Flow Group, Division of Materials Technology, School of Energy and Materials, King Mongkut's University of Technology Thonburi, Bangkok 10140, Thailand

Received 29 August 2005; accepted 11 January 2006

DOI 10.1002/app.24164

Published online in Wiley InterScience (www.interscience.wiley.com).

ABSTRACT: The temperature profiles of wood sawdust/polypropylene (PP) composite melts during cooling were experimentally investigated with a cooling jacket apparatus connected to the end of an injection-molding machine. Real-time melting temperature was measured with an unsheathed thermocouple array coupled with a high-speed data-acquisition unit. The crystallinity level of the solidified composites was evaluated with an X-ray diffractometer. Before the crystallization temperature (T_c) was reached, the cooling rate of the melt layer near the wall was greater than that near the center. After T_c was reached, the opposite behavior was observed. Wood sawdust content did not affect the general temperature and crystallinity profiles across the duct diameter but led to more nonuniform temperature profiles across the duct diameter. The sawdust

particles could act as a nucleating agent during the nucleation stage to increase T_c of the PP and as an interfering agent during the crystal growth stage to decrease the overall crystallinity level of the PP. The temperature and crystallinity profiles were not affected by the coolant flow rate. The normalized induction time changed with reduced radius (r/R , where r is the distance between the central duct to any point along the cross-section of the duct and R is the duct radius) positions and coolant flow rate, especially for neat PP and PP composites with a low sawdust content (10 wt %). © 2006 Wiley Periodicals, Inc. *J Appl Polym Sci* 102: 1896–1905, 2006

Key words: composites; poly(propylene) (PP); processing; thermal properties; thermoplastics

INTRODUCTION

In plastic injection molding, a molten polymer is usually forced via a nozzle into a mold, where it cools and solidifies by dissipating heat through a cooling unit. The cooling stage usually accounts for almost two-thirds of the total cycle time.¹ To reduce the total cycle time, effective heat extraction is then required; this is usually achieved with chilled water as a coolant. A cooling system that provides uniform cooling (and also a uniform rate of cooling) across the molding section is needed to prevent differential shrinkage, warpage, nonuniform crystallinity, and internal stresses in the molding.^{2,3} As a result, a knowledge of changes in melting temperature (T_m) and crystallization behavior of polymer melts during cooling becomes essential.

A number of researchers^{4–6} have examined the temperature and crystallization behaviors of molten polymers during cooling through both computer simula-

tion and experimental approaches. Hu et al.⁴ investigated the effect of cooling system design, part thickness, mold thermal properties, coolant temperature, and cycle time on the cyclic variation of mold temperatures with the dual reciprocity boundary element method. Higher temperature fluctuation was observed near the mold surface. The thermal conductivity and coolant temperature were observed to have a considerable effect on the variations in mold temperature values as compared to effects of cycle time and part thickness. Leephakpreeda⁵ proposed a mathematical model for the solidification of semicrystalline polymers under quiescent nonisothermal crystallization to predict the size of the crystallites. It was suggested that the mean radius of the crystallites was a function of nucleation and growth processes, and the spherulite size increased with increasing cooling rate. Sombatsompop et al.⁶ experimentally studied the temperature gradients of various thermoplastics during the cooling process with a novel temperature-sensing device originally developed by Wood et al.⁷ Their findings suggested that the temperature gradients were influenced by the coolant temperature and crystallization behavior of the polymers used. The work was then extended to investigate the effect of glass-fiber content on the temperature gradient and degree

Correspondence to: N. Sombatsompop (narongrit.som@kmutt.ac.th).

Contract grant sponsor: National Research Council of Thailand.

of crystallinity of polypropylene (PP), and the results suggest that the crystallization process was slowed down by the heat produced inside the polymer sample. The crystallization temperature (T_c) and crystallinity level increased with increasing glass-fiber content. In addition, a simple theoretical model yielded a good comparison with the experimental data at the core part of the molding, with the accuracy more limited at distances away from the center of the mold.⁸ Ota et al.⁹ studied the effects of injection temperature and fiber content on the properties of glass-fiber/PP composites with respect to the density and crystallinity level of the composites. The results showed that increasing glass-fiber content decreased the density and crystallinity level of the composites. Zhu and Edward¹⁰ found that an increase in the injection speed from 2 to 154 mm/s did not lead to any appreciable change in the degree of crystallinity of injection-molded isotactic PP. Xu and Edward¹¹ investigated the effect of a sodium benzoate nucleating agent on the crystalline morphology of PP and found that increases in the crystallinity and spherulite size became less pronounced with increases in the sodium benzoate content.

Natural-fiber-filled polymers have attracted the attention of scientists and technologists over the past few years. Natural fibers, such as wood flour, sisal, flax, bamboo, sun hemp, pineapple, and jute, possess good reinforcing capabilities when properly compounded with polymers. Initially, wood fibers were used for the purpose of disposing of large amounts of natural-fiber waste materials and for cost reduction. They are now preferably being used as reinforcing materials in plastics and offer not only low-cost and low-density in products but also, in many cases, improved mechanical properties that are suitable for structural engineering applications.^{12,13} It is widely known that the properties of these natural-fiber-filled polymer products are directly affected by processing parameters, such as pressure, flow rate, and T_m . T_m during the cooling stage can be regarded as one of the important factors that determine the quality of a polymer product. Nonuniform T_m profiles during cooling may lead to crystallinity and morphology gradients that produce undesirable variations in the mechanical properties of the molded product.

Although the literature has many references⁴⁻¹¹ to the temperature and crystallinity profiles of unfilled and synthetic-fiber-filled thermoplastics during the cooling process, little attention has been given to natural-fiber-filled polymers, especially to research evidence from experiments. Cyras et al.¹⁴ used a non-isothermal kinetic computational model¹⁵ to predict the crystallinity profiles of a sisal-fiber/polycaprolactone/starch molded part. They observed significant differences in temperature and crystallinity gradients at two different positions across the sample

thickness (wall and center), with the results also influenced by the cooling temperature, cooling rate, and sample thickness.

As stated, the experimental data on the effect of cooling on temperature gradients and degree of crystallinity of natural-fiber-filled molten polymers during the cooling process are still limited. This article presents the temperature gradients and degree of crystallinity of wood-sawdust-filled PP melts with a cooling jacket apparatus and an exposed-junction thermocouple temperature sensor. The effects of wood sawdust content and coolant flow rate on the temperature gradients and degree of crystallinity of the wood-sawdust-filled PP composites during cooling were of interest.

EXPERIMENTAL

Raw materials

The polymer used in this work was a PP (Moplen EP310D) supplied in granular form by HMC Polymer Co., Ltd. (Bangkok, Thailand). T_c and T_m of the PP used were determined by a PerkinElmer DSC-7 differential scanning calorimetry (DSC) instrument (Boston, MA); the temperature scanned was from 25 to 200°C with a heating rate of 10°C/min. T_c and T_m of the PP were 115 and 160°C, respectively.

The wood sawdust particles were obtained from carpentry and wood-working processes and supplied by V. P. Wood Co., Ltd. (Bangkok, Thailand). The average size of the sawdust particles used in this study was in the range 100–300 μm . The wood sawdust particles were chemically untreated, and the content added to the PP was varied from 0 to 40 wt %. The sawdust was dried to minimize the moisture content to a known value (5% for this study); the sawdust particles were dried before use through heat treatment in an oven for 24 h at 80°C until the sawdust weight was constant.

Temperature profile measurement

Experimental apparatus

The arrangement of the cooling jacket apparatus used to measure the temperature profiles of the molten sawdust/PP composites during the cooling process is shown in Figure 1; the apparatus was attached to the end of the injection unit of an injection-molding machine (Elite E-80, Italy) with M12 bolts to tightly clamp the components together. The cooling jacket part was made of stainless steel with a water channel around it. A thermocouple sensing array for T_m measurements was inserted between the front and rear sections of the cooling jacket apparatus. The temperature sensor, which was originally invented by Wood et al.,⁷ was based on the use of type K thermocouple

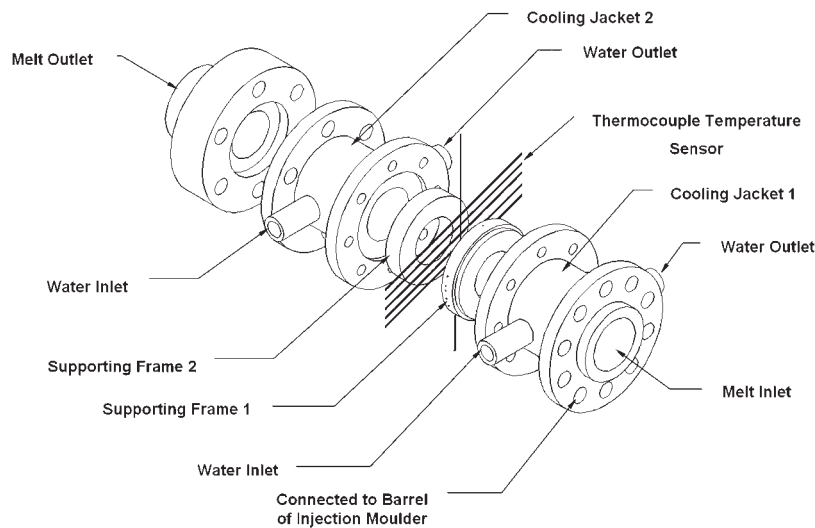


Figure 1 Experimental arrangement of the cooling jacket apparatus for temperature profile measurement during cooling.

wires 0.65 mm in diameter. Because the thermocouple junctions were exposed directly to the molten polymer composites, there was a small error due to the heat conduction and shear heating effects during the temperature measurements. The accuracy of the temperature measurements was on the order of 2.5%. The temperature measurement was taken at different points across the duct diameter of 35 mm; the measured points were 0.0, 3.5, 7.0, 10.5, and 14.0 mm away from the center of the duct, which corresponded to reduced radii (r/R 's, where r is the distance between the central duct to any point along the cross-section of the duct and R is the duct radius) of 0.0, 0.2, 0.4, 0.6, and 0.8, respectively. The temperature measurements were taken with a high-speed data-acquisition card (basic multifunctional DAQ, NI PCI-6013, National Instruments, TX), which was directly connected to a personal computer. The cooling unit was supplied with chilled water, whose temperature was carefully controlled at 10°C throughout this study.

Experimental procedure

The experimental procedure commenced when the apparatus was filled with the composite melt by screw rotation and was left to attain an isothermal equilibrium at an apparatus temperature of 200°C; this took about 30 min.⁸ The chilled water supply was turned on, and the water passed through the cooling jacket of the apparatus. After approximately 5 s, the temperature measurements were started, and composite temperatures across the duct diameter were taken as a function of time. The chilled water was in continuous flow through the apparatus during this period. After 50 min, the chilled water was turned off, and the cooling unit was disassembled. The composite rod was then removed from the

apparatus to measure the crystallinity level. The experiment was then repeated with different wood sawdust contents and coolant flow rates (40, 98, and 143 cm³/s).

Crystallinity profile measurement

The crystallinity level and crystal type of the PP in the wood sawdust/PP composites were measured with an X-ray diffractometer (D8 DISCOVER series 2) for wide-angle X-ray diffraction (XRD), which was supplied by Bruker Advanced X-ray Solutions Co., Ltd. (Karlsruhe, Germany). The equipment settings were 40 mA and 40 kV with a Cu K_α radiation wavelength

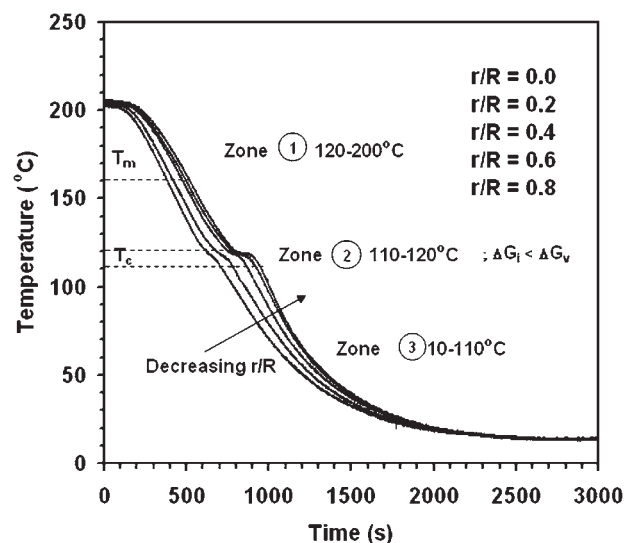


Figure 2 Temperature profiles as a function of time for the neat PP at various r/R positions during cooling with a coolant temperature of 10°C and a coolant flow rate of 40 cm³/s.

of 1.54 Å, and a collection time of 7.5 min. The measurement procedure and calculations of the degree of crystallinity from XRD are described elsewhere.¹¹ The composite rod used for crystallinity measurement was removed after the completion of the cooling of the apparatus. This was possible because the polymer composite contracted under cooling. Small pieces of the polymer at various points across the diameter of the composite rod were taken, and measurements of the degree of crystallinity were then performed by XRD. The radial crystallinity profiles corresponded with the temperature profiles measured during the cooling in the apparatus. The crystallinity profiles of the wood sawdust/PP composites are explained in terms of wood sawdust content and coolant flow rate.

Scanning electron microscopy (SEM) investigations

Failure mechanisms were investigated with a Jeol (JSM-6301F) SEM machine (Tokyo, Japan) at 15 kV

accelerating voltage. The composite fracture surfaces for examination were obtained after 2-min immersions in liquid nitrogen. The details of the experimental procedure and sample preparations were described elsewhere.¹⁶

RESULTS AND DISCUSSION

Temperature profiles

General observations for neat PP

Figure 2 shows the results of the temperature profiles as a function of time for neat PP at various r/R positions across the duct with a coolant temperature of 10°C and a coolant flow rate of 40 cm³/s. Generally, the temperature of the polymer progressively decreased with time. The slope of each curve represented the local rate of cooling of the polymer layers. The cooling rate of the melt layers near the duct wall ($r/R \sim 0.8$) was relatively fast compared with that near the duct

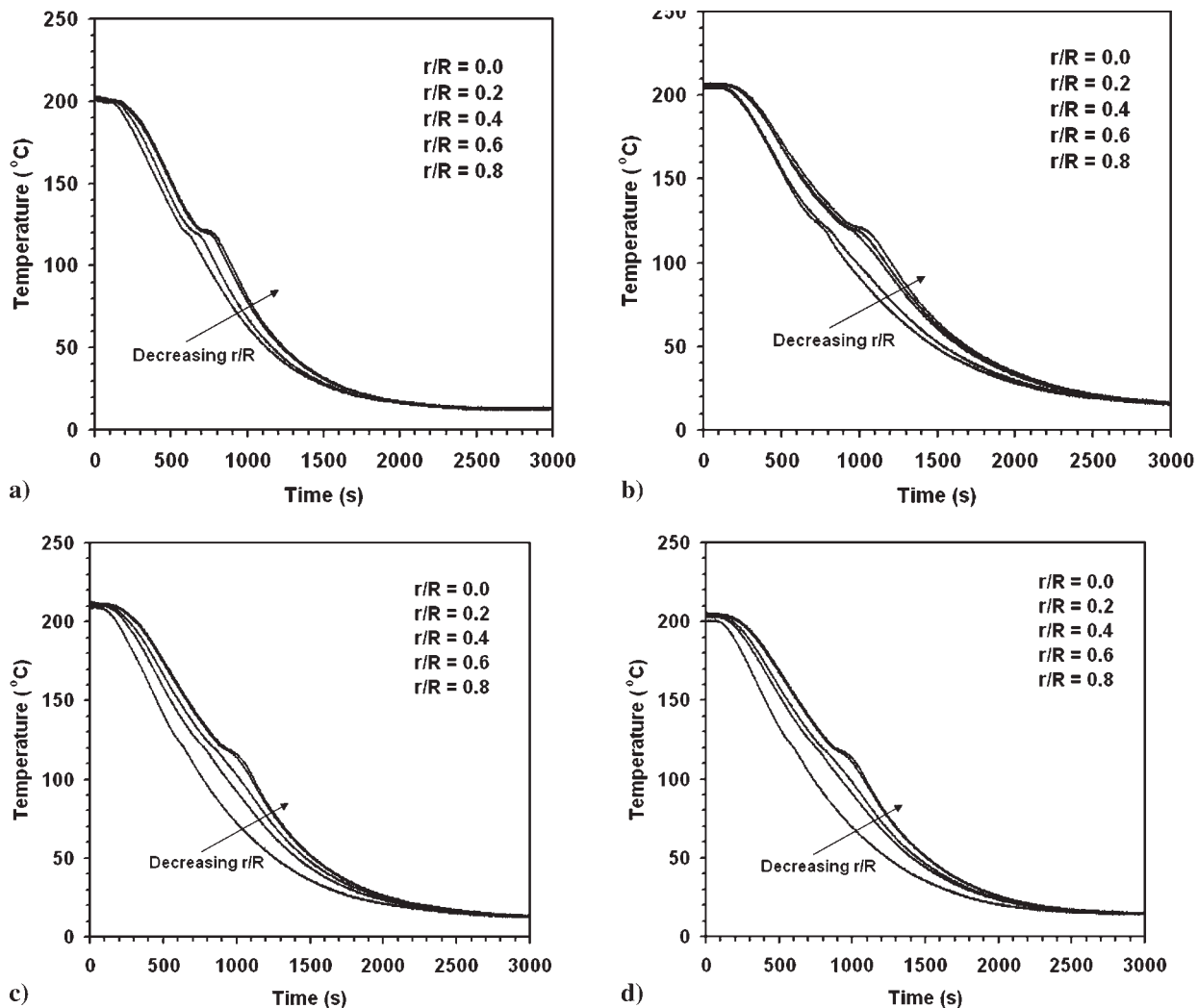


Figure 3 Radial temperature profiles as a function of cooling time for the PP composites with different sawdust contents: (a) 10, (b) 20, (c) 30, and (d) 40 wt %.

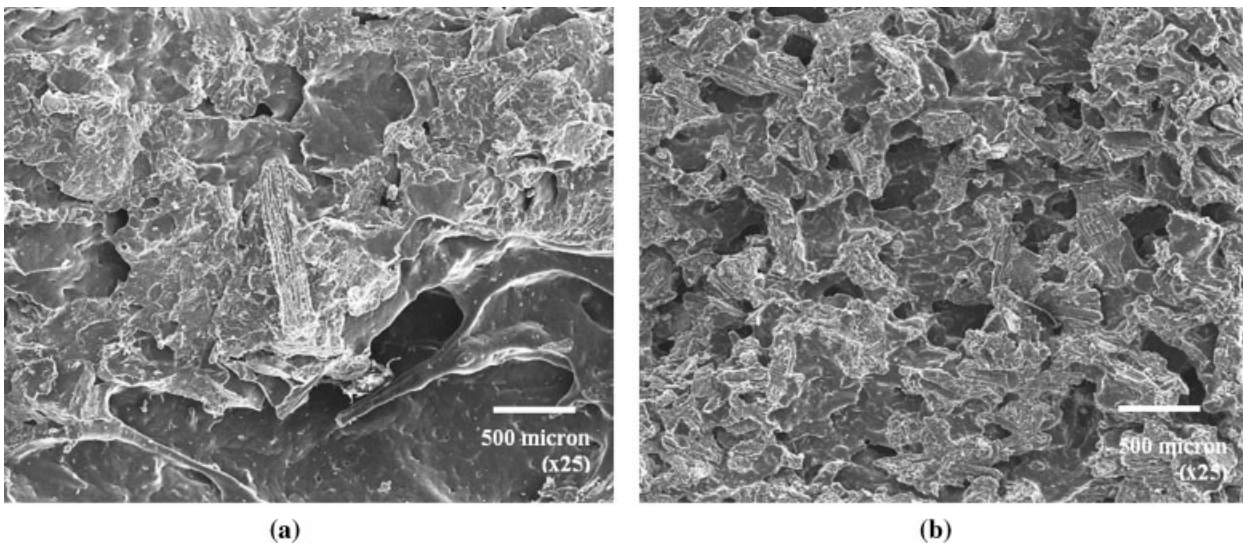


Figure 4 SEM micrographs of the wood sawdust/PP composites: (a) 10 and (b) 40 wt % sawdust.

center. The explanations for the changes in T_m during cooling can be divided into 3 zones as follows:

Zone 1: This is the temperature range 120–200°C, which was referred to as the molten zone of the polymer. In this zone, the local rate of cooling near the duct wall ($r/R = 0.6–0.8$) was higher than at the duct center ($r/R = 0.0–0.2$). This was expected in association with the distances between the melt layers (at the wall and the center) and the cooling wall; a detailed explanation for this was documented elsewhere.^{6,8}

Zone 2: This zone is the temperature range 110–120°C, which was referred to as the crystallizing zone of the polymer. In this zone, plateau values of temperature were observed. The plateau values of temperature were more pronounced around the duct center; this was probably caused by differences in the crystallinity level, which are discussed later. The plateau temperatures were very close to T_c of the polymer. The crystallization mechanism of the PP melt in this zone was referred to as a combination of nucleation and crystal growth processes. The nucleation was endothermic [positive Gibb energy or surface free energy (ΔG_i)], whereas the crystal growth was exothermic [negative Gibb energy or crystallization free energy (ΔG_v)]. During the crystallization, we suggest that ΔG_v was greater than ΔG_i . That is, the plateau values of temperature were caused by an exothermic transformation of the melt during which heat was conducted out due to the change of state; the energy released by the transformation was the dominant factor. This behavior was also found in previous studies.^{6,8}

Zone 3: This zone is the temperature range 10–110°C, which was referred to as the solidifica-

tion zone of the polymer. In this zone, the local cooling rates and their differences for all r/R positions gradually minimized.

Effect of wood sawdust content

The results of the temperature gradient as a function of time at various r/R positions across the duct with a coolant flow rate of 40 cm³/s for the PP composites with different wood sawdust contents (ranging from 10 to 40 wt %) are shown in Figure 3(a–d). The changes in T_m as a function of time and the explanations for the changes were very similar to those for Figure 2. However, a slight difference in the temperature changes among r/R positions as a result of different sawdust contents was observed.

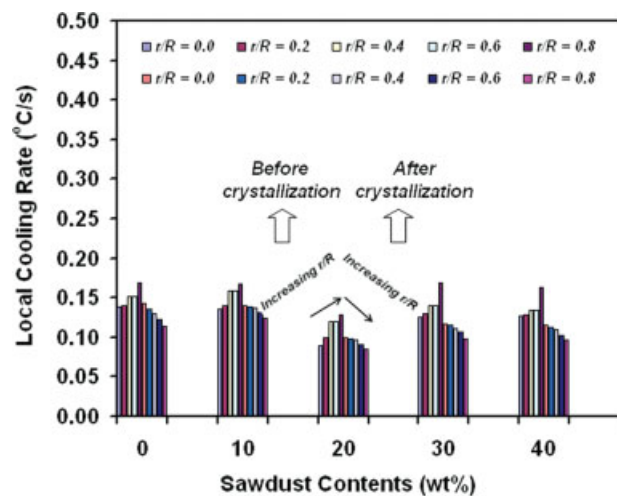


Figure 5 Relationship between the cooling rate and wood sawdust content of the wood sawdust/PP composites at various r/R positions during cooling. [Color figure can be viewed in the online issue, which is available at www.interscience.wiley.com.]

That is, the greater the wood sawdust content was, the more pronounced the temperature difference was among r/R positions. This probably involved two possible reasons: one was the sawdust distribution, and the other involved voids as a result of increasing wood sawdust particles in the PP matrix. With regard to the first reason, the sawdust particles in the PP matrix preferred to cling together due to hydrogen bonds in the molecules.¹⁶ Figure 4 shows the SEM micrographs of the PP composites with 10 and 40 wt % wood sawdust particles. The sample with 40 wt % sawdust had more voids in the PP matrix, which resulted in more discontinuous phases in the composites and, thus, larger temperature differences across the duct diameter (r/R positions).

For comparison purposes, the temperature profile results in Figure 3 were then replotted in terms of the local cooling rate ($^{\circ}\text{C}/\text{s}$) for the selected temperature

ranges $120\text{--}150^{\circ}\text{C}$ (before crystallization) and $60\text{--}80^{\circ}\text{C}$ (after crystallization); this is shown in Figure 5. Before crystallization, the local cooling rate near the duct wall was greater than near the duct center. Before crystallization, the polymer was in the molten stage, and the melt was cooled down by a combination of conduction and convection effects. The combined heat-transfer effects were relatively pronounced for the melt located near the duct wall, and thus, a faster cooling rate was observed. This implied a lower crystallinity level of the PP near the duct wall, with a higher degree of crystallinity near the duct center. After crystallization, the polymer was in the solid stage, and the cooling was mainly caused by the conduction effect; the ability of the heat to transfer became very much dependent on the crystallinity level. It is expected that the crystallinity level of the polymer at the center was greater due to the slower cooling rate at

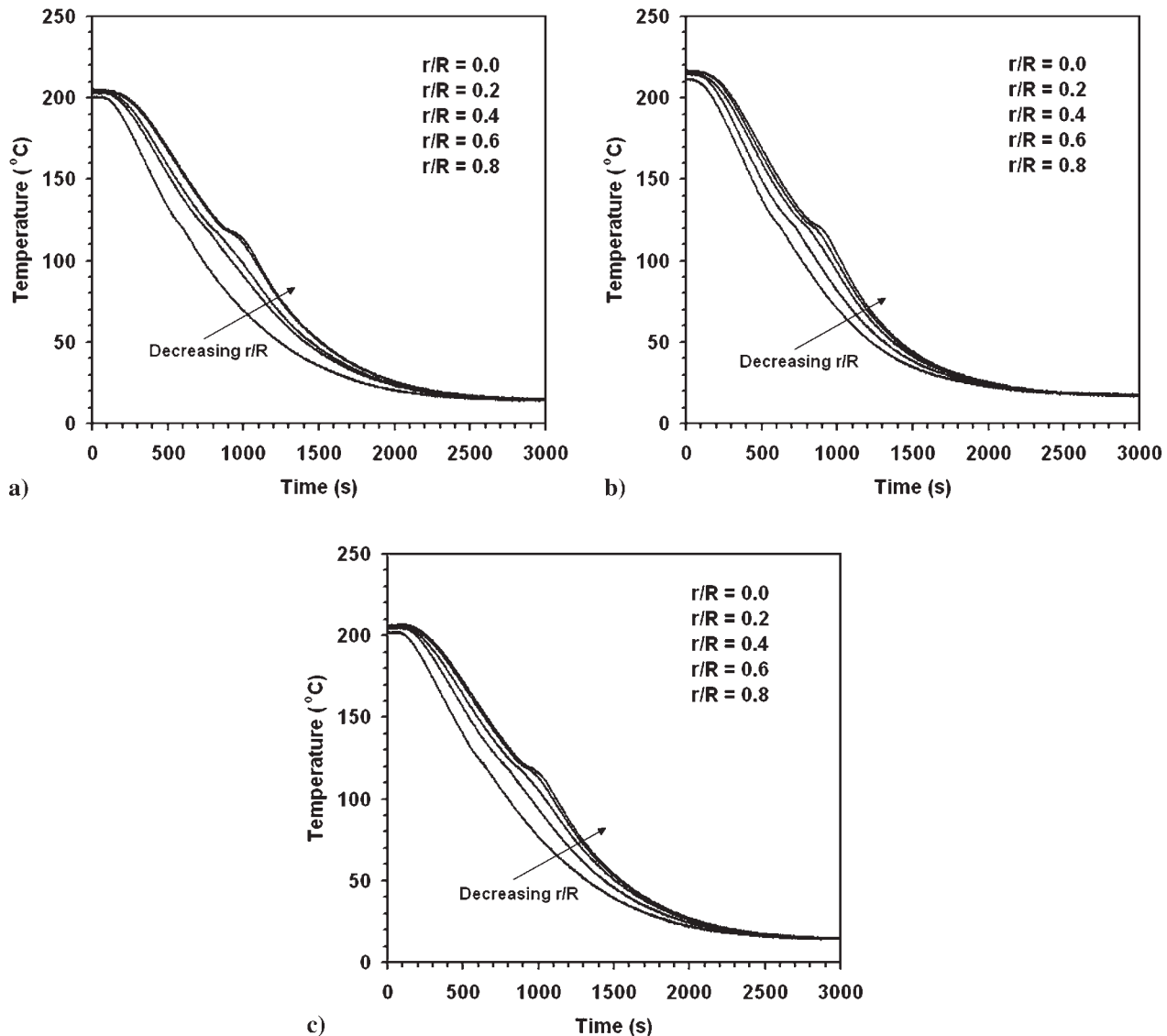


Figure 6 Radial temperature profiles as a function of time for the PP composite with 40 wt % wood sawdust for different coolant flow rates: (a) 40, (b) 98, and (c) $143\text{ cm}^3/\text{s}$.

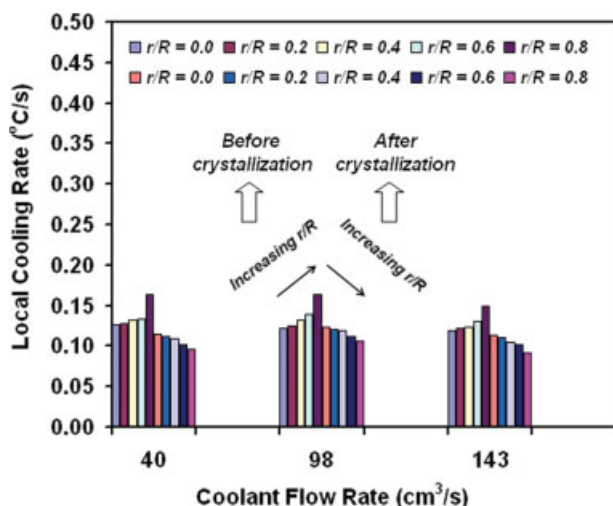


Figure 7 Relationship between cooling rate and coolant flow rate of the PP composite with 40 wt % wood sawdust at various r/R positions during cooling. [Color figure can be viewed in the online issue, which is available at www.interscience.wiley.com.]

the crystallization stage. This was why the local cooling rate of the polymer at the duct center after the crystallization stage was greater, as shown in Figure 5. The wood sawdust content did not have an obvious effect on the local cooling rate of the melt.

Effect of coolant flow rate

We selected the PP composite with 40 wt % wood sawdust to study the effect of the coolant flow rate on the temperature profiles as a function of time across

r/R positions; the results are shown in Figure 6(a–c). It was expected that the greater the coolant flow rate was, the higher the local cooling rate of the polymer (steeper temperature gradient) and the smaller the temperature step during the crystallizing zone would be. However, this behavior could not be clearly seen, as shown in Figure 6(a–c). In this respect, the temperature profile results were then replotted in terms of the local cooling rate ($^{\circ}\text{C}/\text{s}$) for the selected temperature ranges 120–150 $^{\circ}\text{C}$ (before crystallization) and 60–80 $^{\circ}\text{C}$ (after crystallization), as shown in Figure 7. The explanations for the changes in the local cooling rate at various r/R positions before and after crystallization were similar to those mentioned for Figure 5. Similar to the effect of wood sawdust content, the coolant flow rate did not have an obvious effect on the local cooling rate of the melt.

Crystallinity analysis

Effect of wood sawdust content

Figure 8 shows the XRD patterns of the solidified PP rod taken at the center position of sample; different wood sawdust contents were cooled from 200 to 10 $^{\circ}\text{C}$ in the cooling jacket apparatus with a coolant flow rate of 40 cm^3/s . There were two different crystal types, which were the monoclinic type (axis $a \neq b \neq c$ and angle $\alpha = \gamma = 90^{\circ}$, $\beta \neq 90^{\circ}$) and the hexagonal type (axis $a = b \neq c$ and angle $\alpha = \gamma = 90^{\circ}$, $\beta = 120^{\circ}$), and the Miller indices corresponding to the XRD planes were $\alpha_1(110)$, $\alpha_2(040)$, $\alpha_3(130)$, $\alpha_4(041)$, $\alpha_5(060)$, and $\beta(300)$.^{10,11} To analyze the crystal type influenced by the wood sawdust content, we

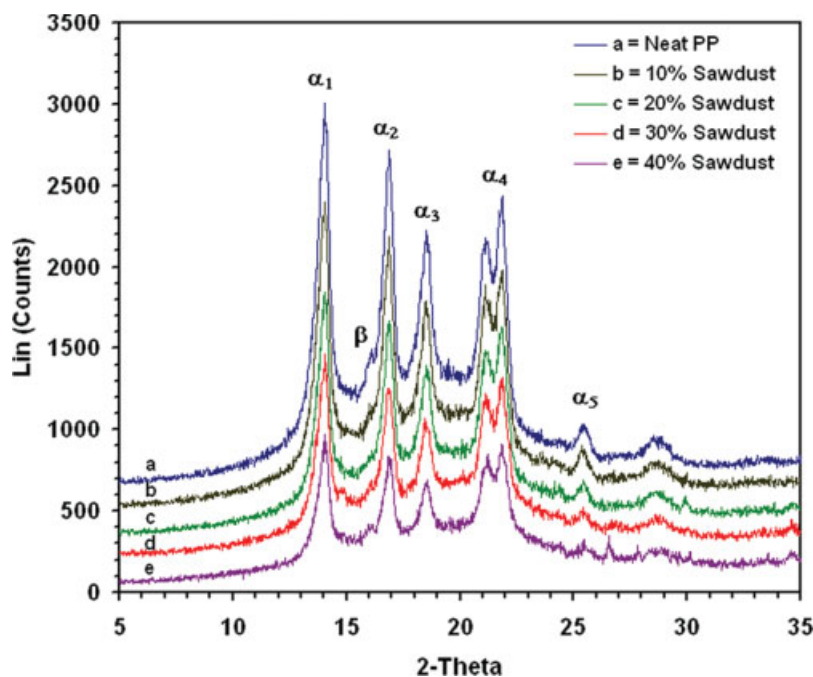


Figure 8 XRD patterns of the PP composites with different wood sawdust contents during cooling. [Color figure can be viewed in the online issue, which is available at www.interscience.wiley.com.]

TABLE I
 T_m and T_c Values of the PP composites with Different Wood Sawdust Contents as Measured by DSC

Wood sawdust content (wt %)	T_m (°C)	T_c (°C)	T_c range (°C)
0	164	114	111–121
10	163	117	113–121
20	164	117	114–121
30	164	118	115–122
40	164	118	116–122

considered the height of the α_2 peak at 16.2° and the appearance of the $\beta(300)$ peak at 16.9°. As the wood sawdust content increased, the height of all α peaks decreased dramatically; this indicated that the crystallinity level of the PP decreased with increasing sawdust content. The decrease in the crystallinity level of glass-fiber-filled PP was also evidenced by Ota et al.⁹ However, the β peak, which was referred to as a transcrystalline structure, could be assessed by the ratio of the height of $\beta(300)$ reflection to the sum of the height of all of the α and β peaks.¹⁷ The β fraction from the composite sample increased with increasing sawdust content.

Table I shows the T_m and T_c values from the DSC technique for the PP composites with wood sawdust particles ranging from 0 to 40 wt %. T_m of the composites remained unchanged, whereas T_c increased with increasing sawdust content. The increase in T_c suggested that the sawdust particles probably acted as a nucleating agent, which restricted the molecular mobility of the polymer chains and then caused the polymer to crystallize (nucleation stage) at a higher temperature on cooling. However, as shown in Table I, we also found that the T_c range was narrower as the sawdust content was increased. This implied that the sawdust particles could act as an interfering agent during the crystal growth. If this was the case, the crystallinity level of the sawdust/PP composites was expected to decrease with sawdust content. Table II shows the results of the degree of crystallinity from the XRD patterns at various r/R positions across the duct for the PP composites with wood sawdust particles ranging from 0 to 40 wt %. An increase in wood sawdust particles in the PP resulted in a progressive decrease in the degree of

TABLE II
Degree of Crystallinity (%) of the PP Composites with Different Wood Sawdust Contents as Measured by XRD

r/R	Wood sawdust content (wt %)				
	0	10	20	30	40
0.0	34.9	32.9	31.0	28.0	25.9
0.2	34.4	32.8	29.7	27.0	26.3
0.4	34.4	31.2	29.3	27.5	25.5
0.6	34.3	32.2	29.3	26.1	26.9
0.8	33.6	31.8	29.9	25.5	26.0

TABLE III
Degree of Crystallinity of the Neat PP for Various Coolant Flow Rates

r/R	Coolant flow rate (cm ³ /s)		
	40.0	98.3	143.3
0.0	34.9	37.4	37.6
0.2	34.4	36.2	34.7
0.4	34.4	35.4	36.1
0.6	34.3	35.2	35.8
0.8	33.6	34.0	34.2

crystallinity of the polymer. This behavior was also found by Ota et al.⁹ We concluded that the decrease in the crystallinity level of the PP was due to that the wood sawdust particles interfering with the growth of the PP crystals during crystallization, although the sawdust particles acted as a nucleating site in the composites during the nucleation stage. Table II also shows the change in the crystallinity level at various r/R positions across the duct diameter. There was no difference in the degree of crystallinity across the duct diameter because of the relatively small different local cooling rates of all of the r/R positions, as already shown in Figure 5. This was also found in our previous work⁸ and in work by Zhu and Edward.¹⁰

Effect of coolant flow rate

Tables III and IV show the results of the degree of crystallinity from XRD for neat PP and the 40 wt % sawdust/PP composite, respectively, with different coolant flow rates at various r/R positions across the duct. Again, the overall crystallinity level for the PP composite was greater than that for neat PP. The coolant flow rate had no effect on the degree of crystallinity across the duct diameter (r/R positions) for both PP samples because of small differences in the local cooling rates, as mentioned earlier.

Although the temperature and crystallinity profiles of the PP in the sawdust/PP composites in this study did not change with coolant flow rate, the induction time,¹⁸ which was defined in this work as the time from T_m (200°C) to T_c (115°C), was affected by the coolant flow rate. The induction time is very important when polymer products are manufactured

TABLE IV
Degree of Crystallinity of the PP Composite with 40 wt % Sawdust for Various Coolant Flow Rates

r/R	Coolant flow rate (cm ³ /s)		
	40.0	98.3	143.3
0.0	25.9	25.5	28.7
0.2	26.3	25.3	26.1
0.4	25.5	25.0	27.0
0.6	26.9	24.0	25.4
0.8	26.0	23.3	25.9

because it influences the total production time.¹⁹ A minimal induction time is usually required for effective productivity and cost-saving processes. Figure 9 shows the effect of coolant flow rate on the induction time as a function of r/R positions of the PP composites with different wood sawdust contents. For comparison purposes, the induction time in this study was considered in terms of normalized values, which were referred to as the ratio of the actual to the minimum induction time value. In all cases, the induction time of the PP at the duct center was relatively longer than that near the wall, as expected. Both the wood

sawdust content and coolant flow rate had significant effects on the induction time. The normalized induction time decreased with increasing wood sawdust content (Fig. 9). This was expected because an increase in the sawdust particles tended to increase the thermal conductivity of the composites, which probably improved the heat conduction effect.²⁰ The coolant flow rate had a more pronounced effect on the induction time for neat PP and the 10 wt % sawdust/PP samples; the effect of the coolant flow rate was insignificant at high sawdust contents (20 and 40 wt %). We were surprised to note that the relationship

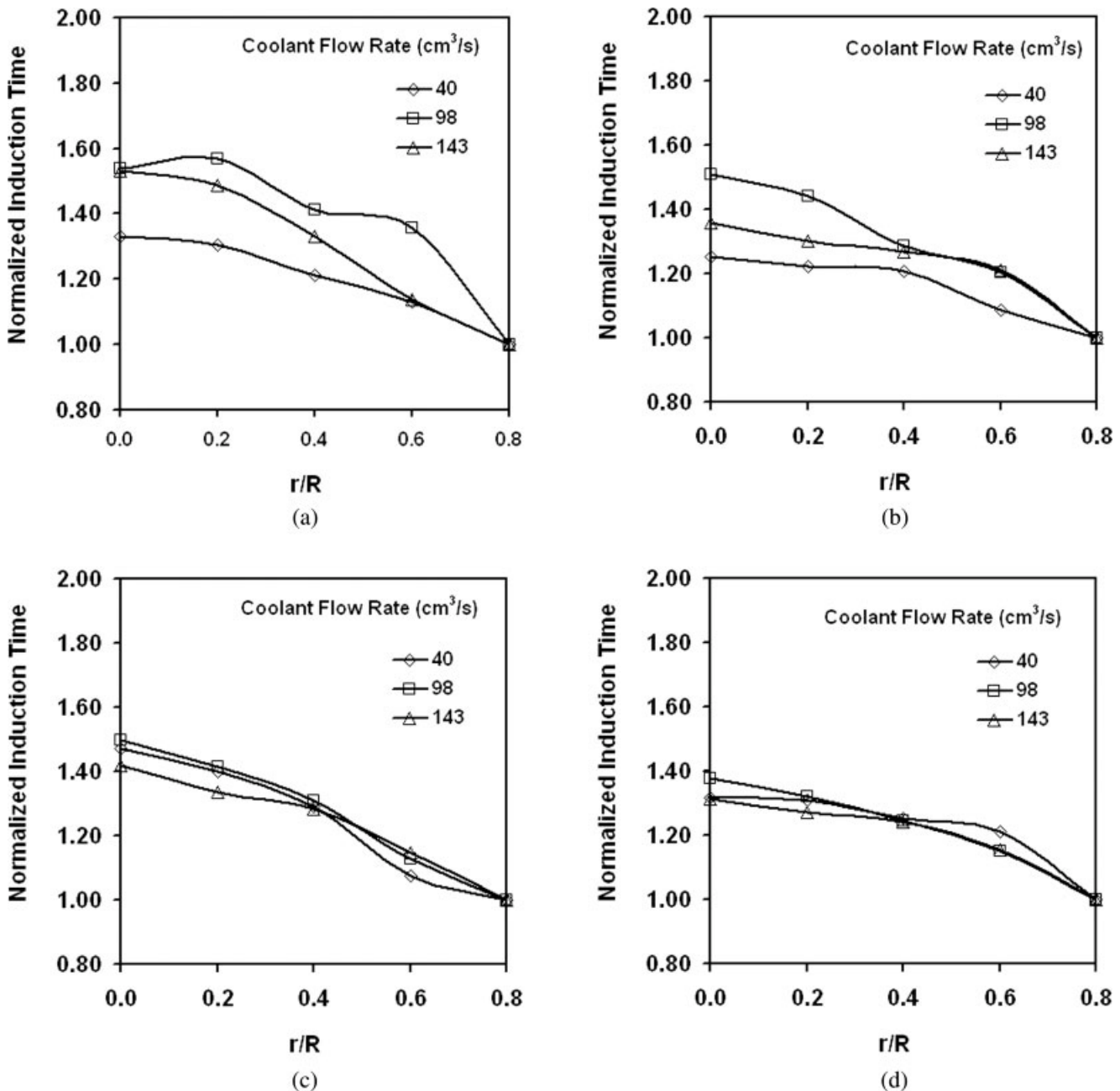


Figure 9 Normalized induction time as a function of r/R position across the duct for different coolant flow rates and wood sawdust contents: (a) 0, (b) 10, (c) 20, and (d) 40 wt %.

between the coolant flow rate and the induction time was not linear; the minimum and maximum induction times were at coolant flow rates of 40 and 98 cm³/s, respectively. The reason for this can be explained by the flow pattern of the coolant, which could be predicted through the Reynolds number (N_{Re}) as calculated with eq. (1):²¹

$$N_{Re} = \frac{(D_2 - D_1)G}{\mu} \quad (1)$$

where G is the mass flow rate per unit area of flow (varied by the coolant flow rate), μ is the viscosity of the coolant (1×10^{-2} g cm⁻¹ s⁻¹), and D_1 and D_2 are the inner (3.9 cm) and outer (6.0 cm) diameters of the duct.

In this study, the calculated N_{Re} 's of the coolant flow rates at 40, 98, and 143 cm³/s were 1600, 3933, and 5733, respectively. Work by Xie et al.²¹ suggested that fluids with N_{Re} 's from 900 to 2000 exhibited a laminar character, whereas those with N_{Re} 's from 12,000 to 220,000 showed a turbulent character. In relation to this study, the N_{Re} of 1600 (40 cm³/s) clearly indicated a laminar flow of the coolant, whereas those of 3933 and 5733 probably indicated a transient flow with a vortex characteristic in the flow channel. The vortex flow was evidenced to affect the heat convection of the fluid; greater vortex flows led to a reduction in the convective heat-transfer coefficient.²¹ In relation to this study, the vortex-contained laminar flow for the coolant flow rate of 98 cm³/s probably resulted in a reduction of heat-transfer effectiveness between the coolant and the melt. In the case of the 143 cm³/s coolant flow rate, the vortex flow was probably minimized by an increase in the degree of turbulence to the coolant flow; this was believed to improve the effectiveness of the heat transfer between the coolant and the melt and, thus, to decrease the induction time. This explanation was in line with that proposed by Xie et al.²¹

CONCLUSIONS

In this study, we examined the effects of wood sawdust content and coolant flow rate on the temperature and crystallinity profiles across the duct diameter of molten wood sawdust/PP composites during cooling. The following are noted:

1. T_m of the PP decreased with time. Before crystallization, the cooling rate of the melt layer near the duct wall was greater than that near the duct center. After crystallization, the effect was the opposite.
2. The increase of wood sawdust content had no effect on the general patterns of the temperature and crystallinity profiles across the duct diameter of the PP. An increase in wood sawdust content resulted in more nonuniform temperature profiles across the duct diameter.

3. The sawdust particles acted as a nucleating agent in the PP matrix during the nucleation stage, which resulted in an increase in T_c with increasing sawdust content. However, the sawdust particles interfered with the crystallization during the crystal growth and resulted in a decrease in the overall crystallinity level of the PP with increasing sawdust content.
4. An increase in the coolant flow rate had no effect on the temperature and crystallinity profiles but had a strong effect on the induction time, especially for neat PP and the PP composite with a low sawdust content (10 wt %).

NOMENCLATURE

ΔG_i	Surface free energy (N m)
ΔG_v	Crystallization free energy (N m)
μ	Coolant viscosity (kg m ⁻¹ s ⁻¹)
D_1	Inner diameter of the duct (m)
D_2	Outer diameter of the duct (m)
G	Mass flow rate (kg/s)
N_{Re}	Reynolds number
r	Distance between the duct central to any point along the cross-section of the duct (m)
R	Duct radius (m)
T_c	Crystallization temperature (°C)
T_m	Melting temperature (°C)

References

1. Li, C. L.; Li, C. G.; Mok, A. C. K. *Comput-Aided Des* 2005, 37, 645.
2. Crawford, R. J. In *Plastics Engineering*; Pergamon: Oxford, 1987.
3. Agassant, J.-F.; Avenas, P.; Sergent, J.-P.; Carreau, P. J. In *Polymer Processing: Principles and Modeling*; Hanser: New York, 1991.
4. Hu, S. Y.; Cheng, N. T.; Chen, S. C. *Plast Rubber Compos Process Appl* 1995, 23, 221.
5. Leephakpreeda, T. *ScienceAsia* 2001, 27, 127.
6. Sombatsompop, N.; Chonniyom, D.; Wood, A. *J Appl Polym Sci* 1999, 74, 3268.
7. Wood, A. K.; Judeh, Y.-H.; Yue, M. *Brit. Pat. GB 2291197* (1996).
8. Sombatsompop, N.; Tangsongcharoen, A. *J Appl Polym Sci* 2001, 82, 2087.
9. Ota, W. N.; Amico, S. C.; Satyanarayana, K. G. *Compos Sci Technol* 2005, 65, 873.
10. Zhu, P. W.; Edward, G. *Macromol Mater Eng* 2003, 288, 301.
11. Xu, T.; Lei, H.; Xie, C. S. *Mater Des* 2003, 24, 227.
12. Roberts, J. C.; Boyle, M. P.; Wienhold, P. D.; White, G. J. *Compos B* 2002, 33, 315.
13. Carroll, D. R.; Stone, R. B.; Sirignano, A. M.; Saindon, R. M.; Gose, S. C.; Friedman, M. A. *Resour Conserv Recycl* 2001, 31, 241.
14. Cyrus, V. P.; Stefani, P. M.; Ruseckaite, R. A.; Vazquez, A. *Polym Compos* 2004, 25, 461.
15. Kamal, M. R.; Chu, E. *Polym Eng Sci* 1983, 23, 27.
16. Sombatsompop, N.; Chaochanchaikul, K.; Phromchirasuk, C.; Thongsang, S. *Polym Int* 2003, 52, 1847.
17. Wang, W.; Tang, L.; Qu, B. *Eur Polym J* 2003, 39, 2129.
18. Sudduth, R. D.; Yarala, P. K. *Polym Eng Sci* 2002, 42, 694.
19. Park, S. J.; Kwon, T. H. *Polym Eng Sci* 1998, 38, 1450.
20. Sombatsompop, N.; Wood, A. K. *Polym Test* 1997, 16, 203.
21. Xie, W.; Tam, S. C.; Yang, H.; Gu, J.; Zhao, G.; Lam, Y. L.; Kam, C. H. *Opt Laser Technol* 1999, 31, 387.